Published in final edited form as:
Nanotechnology. 2008 August 20; 19(33): 335601. doi:10.1088/0957-4484/19/33/335601.

Synthesis and characterization of ultra-small superparamagnetic iron oxide nanoparticles thinly coated with silica

A Bumb[1,2], **M W Brechbiel**[2], **P L Choyke**[3], **L Fugger**[4], **A Eggeman**[5], **D Prabhakaran**[6], **J Hutchinson**[6], and **P J Dobson**[1,7]

[1] Oxford University Begbroke Science Park, Sandy Lane, Kidlington, Oxon OX5 1PF, UK. Email: Ambika.Bumb@eng.ox.ac.uk, Peter.Dobson@begbroke.ox.ac.uk

[2] Radioimmune & Inorganic Chemistry Section, Radiation Oncology Branch, NCI, NIH, Building 10, Room 1B40, 10 Center Drive, Bethesda, MD 20892, USA

[3] Molecular Imaging Program, NCI, NIH, Building 10, Room 1B40, 10 Center Drive, Bethesda, MD 20892, USA

[4] RC Human Immunology Unit, Weatherall Institute of Molecular Medicine, John Radcliffe Hospital, The University of Oxford, Oxford OX3 9DS, UK

[5] Department of Materials, University of Oxford, Parks Road, Oxford OX1 3PH, UK

[6] Department of Physics, University of Oxford, Parks Road, Oxford OX1 3PH, UK

Abstract

Ultra-small superparamagnetic iron oxide nanoparticles (SPIOs) were synthesized by co-precipitation of iron chloride salts with ammonia and then encapsulated with thin (~2nm) layers of silica. The particles have been characterized for size, diffraction pattern, surface charge, and magnetic properties. This rapid and economical synthesis has a number of industrial applications; however, the silica-coated particles have been optimized for use in medical applications as MR contrast agents, biosensors, DNA capturing, bioseparation and enzyme immobilization

1. Introduction

At the boundary between nanomaterials and medical diagnostics, superparamagnetic iron oxide nanoparticles (SPIOs) are proving to be a class of novel probes useful for *in vitro* and *in vivo* cellular and molecular imaging. The face-centered cubic packing of oxygen in maghemite/magnetite, γ-Fe_2O_3/Fe_3O_4, allows electrons to jump between iron ions occupying interstitial tetrahedral and octahedral sites, thus giving the molecules half-metallic properties that are suitable for magnetic resonance imaging (MRI) [1]. Along with providing MR contrast, SPIOs present unique properties that can be applied in targeted delivery of therapeutic agents, development of immunochromatographic tests, localized thermotherapy (i.e. hyperthermia), and conversion of a pro-drug to its active form [2]. Unlike many nanoprobes, iron-based nanoparticles have a well recognized metabolic fate *in vivo* that has been accepted by regulatory agencies.

Two key factors play an important role for *in vivo* applications of these particles: size and surface functionality. Even without targeting surface ligands, SPIO diameter greatly affects *in vivo* biodistribution. Larger particles with diameters ranging from 300nm to 3.5μm that are

[7] Author to whom any correspondence should be addressed.

coated with an insoluble layer are highly effective at imaging the gastrointestinal tract [3]. Particles from 60 to 150nm are taken up by the reticuloendothelial system leading to rapid uptake in the liver and spleen [4]. Particles with diameters of 10 to 40 nm, including ultrasmall SPIOs (USPIOs), are optimal for prolonged blood circulation, can cross capillary walls, and are often phagocytosed by macrophages which traffic to lymph nodes, and bone marrow [4].

Particle interactions with their environment are greatly affected by surface functionality. Silica is a biocompatible material suitable for preserving the intrinsic properties of USPIO cores by preventing degradation and aggregation of the inner Fe_2O_3/Fe_3O_4 core. Immobilization of the iron oxide allows for tailoring of the particles by straightforward linkage of functional groups to surface silanol groups that exist as a consequence of silica encapsulation. Silanols easily react with alcohols and silane coupling agents [5] to produce dispersions that are stable in non-aqueous solvents and are ideal for strong covalent bonding with ligands such as biomolecules or drugs. The silanol groups also make particle surfaces lyophilic, conferring enhanced stability for particle suspensions during changes in pH or electrolyte concentration [6]. Optically transparent [7], silica is heat-resistant, has low specific gravity, and good mechanical strength. An additional advantage silica offers for biomedical application is the tunable thickness of the applied encapsulation layer. Optimized for this purpose, 9nm USPIOs coated with 2–5nm thin layers of silica have been synthesized and characterized. Herein, their preparation and fundamental properties are reported.

2. Synthesis

Precipitation-based methods, such as co-precipitation of metal salts [8,9] or reverse micelle synthesis [10,11] are most commonly used to synthesize SPIOs. Though reverse micelle synthesis can produce very uniform particles, they are soluble only in organic solvents. Therefore, for medical applications, co-precipitation is the more preferred route of synthesis. Herein, USPIOs were synthesized by co-precipitation of ferrous and ferric salts in alkaline and acidic aqueous.

As described in the LaMer diagram (figure 1) [12], for homogeneous precipitation, as concentration increases to past saturation, a point is reached where nucleation occurs. Particle growth most likely transpires by a combination of diffusion of atoms onto nuclei and irreversible aggregation of nuclei. In order to produce monodisperse particles, the rate of nucleation must be high and τ short, to generate a burst of nuclei. The rate of growth of the nuclei must be fast enough to reduce the concentration below the nucleation concentration to limit the number of particles created. The low surface energy of iron oxide increases the driving force for nucleation and thus a large number of nuclei are formed.

With a stoichiometric ratio of $2Fe^{3+}$:Fe^{2+}, 16mmol (4.43g) FeCl3·6H2O and 8mmol (1.625g) of FeCl2·4H2O were dissolved in 190mL deionized water at room temperature by magnetic stirring in a beaker.

$$2Fe^{3+}(aq)+Fe^{2+}(aq) \xrightarrow{OH^-} Fe_3O_4(c) \quad (1)$$

Under conditions of vigorous stirring, 10mL of 25% NH_3 was poured down the vortex of the iron solution. Immediately, magnetite formed a black precipitate. After stirring for ten minutes, the particles were washed thrice with water by magnetic separation. In order to stabilize the particles in solution, they were surface-complexed with citrate ions by means of the following process: First, the particle surface was converted from negative to positive by washing twice with 2M HNO_3. These acid washes not only reversed the zeta potential of the magnetite colloid

and removed any remaining ammonium ions, but also caused the material to release Fe^{2+}, converting the magnetite to maghemite, with no reduction in particle size [13]:

$$(Fe_8^{3+})_{tet}(Fe_8^{3+}Fe_8^{2+})_{oct}O_{32} \xrightarrow{H^+} \frac{3}{4}(Fe_8^{3+})_{tet}(Fe_{\frac{40}{3}}^{3+}[\,]_{\frac{8}{3}})_{oct}O_{32}+8H_2O+8Fe^{2+} \quad (2)$$

Leaching of Fe^{2+} was noted by the change in supernatant color to a rusty yellow. Typically, the protocol for stabilization with citrate was continued by raising the pH to 2.5 with NaOH. While maintaining ~pH 2.5 with perchloric acid, a volume of 5mL of 0.5M $Na_3[C_3H_5O(COO)_3]$ solution was added and the solution stirred for 1.5 hr. The particles were washed with DI water and diluted to 50mL (~pH 6) for a final concentration of 30nmol NP/mL. The final citrate-complexed USPIOs were quite stable at this pH because the unadsorbed carboxylate groups of the weakly acidic citrate are deprotonated[14] (figure 2).

A number of different techniques have previously been used to coat iron oxide with silica. Zhang and coworkers[15] used an in situ reverse microemulsion micelle synthesis method to generate silica-coated magnetite particles dispersed in an organic solvent, while Homola[16] reported a method that used Ludox silica particles, a colloidal silica suspension, to coat iron oxide. Woo et al[17] employed a technique of magnetite treatment with toluene, ammonium hydroxide, and ethanol followed by the addition of tetraethylorthosilicate (TEOS) for 1 day. The solution was then heated to 150°C for 1 h and cooled before 3-aminopropyltrimethoxysilane was added and again the solution was heated to 150°C for 1 h and cooled. After treatment with excess ethanol and separation by centrifugation, the solid yield was of silica-coated magnetite particles with surface propylamine functional groups.

Herein, the simpler Stöber method, developed by Stöber, Fink, and Bohn in 1968 [18], was used to coat USPIOs with silica and leave them dispersed in aqueous solution. This mechanism involves hydrolysis of an alkoxy silane and condensation of alcohol and water [19]:

$$\equiv Si-OR+H_2O \;\leftrightarrow \equiv Si-OH+ROH \quad (3)$$

$$\equiv Si-OR+\equiv Si-OH \;\leftrightarrow \equiv Si-O-Si\equiv +ROH \quad (4)$$

$$\equiv Si-OH+\equiv Si-OH \;\leftrightarrow \equiv Si-O-Si\equiv +H_2O \quad (5)$$

Particle synthesis can be controlled ranging from formation of large silica spheres embedded with a number of USPIOs down to single USPIOs coated with very thin layers of silica. The following protocol was optimized for 2 to 3.5nm thick coatings around single USPIOs. In a typical synthesis, 30nmol of USPIO were sonicated in 2.5mL DI water for 10 min to ensure even distribution and prevent aggregation. A volume of 250μL TEOS was injected into 2.25mL of ethanol and this solution was added to the USPIO solution. To catalyze the reaction, 100μL of triethylamine were added. The reaction was run under sonication for 15 min and then washed by magnetic separation with DI water. This procedure is reproducible and can be reasonably scaled as long as solvent and reagent ratios are kept constant.

3. Characterization

3.1. Transmission Electron Microscopy

Using transmission electron microscopy (JEOL 4000EX), both bare USPIO and silica-coated USPIOs were analyzed (figure 3). Multiple samples of both types were drop-cast onto carbon grids. A particle's diameter was determined as the mean of three cross-sectional measurements. Analyses of repeated syntheses yielded that the USPIO diameter had a lognormal distribution, as is typical with such crystals[20], where the geometric mean diameter was 9.2nm (s_{geo} =1.1nm). Thickness measurements of the silica layers were used to determine the optimal protocol to generate shells as thin as 2nm.

Diffraction patterns of the core USPIO and its surrounding silica shell were obtained to analyze the crystalline structure of the materials. As would be expected by the fcc packing of iron oxide crystals, all the diffraction rings *h*,*k*,*l* are either all even or all odd, where zero is considered even. Based on the diffraction rings, the core structure was confirmed to be magnetite or maghemite and that TEOS was condensed on the USPIO surface as silicon (IV) oxide.

3.2. Zeta Potential

Characterizing the particle surface properties is necessary to understand and predict properties under physiological conditions and also to optimize conjugation chemistry. Surface charge was characterized by zeta (ζ) potential analysis with a Malvern ZetaMaster and Nanosizer. The isoelectric point, also referred to as PZC (point of zero charge), is the pH at which the particles in suspension have a net charge of zero and no mobility in the electric field. Samples were analyzed for ζ-potential and the results are presented in figure 5. Adjustments in pH were made with ammonia, potassium hydroxide, hydrochloric acid, and nitric acid. USPIOs that were only washed with nitric acid showed partial conversion to maghemite as is evident by the dip in ζ-potential near pH 5. By re-characterizing surface charge after allowing the particles to sit in nitric acid for 5 days for full conversion of magnetite to maghemite, the PZC of maghemite was confirmed to be lower than magnetite. Silica coating made the sol anionic across the working pH range. The stable negative charge in the pH range of 6–7 is desirable because this mimics the negative charge of most biomolecules in physiological conditions [21]. In stable pH range of above 5, the dynamic light scattering (DLS) determined hydrodynamic diameter of silica-coated USPIOs was 18nm, comparable to TEM measurements.

3.3. Magnetic Properties

Sample solutions of USPIOs and silica-coated USPIOs were dried to solid form in a SpeedVac. A mass of 25.5 mg of each sample was collected for analysis using a superconducting quantum interference device (SQUID) (Quantum Design MPMS XL). To confirm that the particles were in fact superparamagnetic, hysteresis curves were analyzed. Magnetic domains of ferromagnetic materials have a magnetic memory where once aligned in an applied field, they do not return to their original state without expenditure of energy. This dependency on recent history traces a hysteresis loop and energy loss is measured by the area of the loop. Superparamagnetic materials have no permanent magnetic moment and, hence, no hysteresis loop. To test the magnetic behavior of the two samples, the temperature was held constant at 100K and 310.15K (body temperature) for hysteresis measurements in two applied field ranges: ±7T and ±0.01T (figure 6). The shape of the hysteresis curve for both samples at both temperatures under high applied field (figures 6A&6C) was normal and tight with no hysteresis losses, as is expected behavior for a superparamagnet. Under low applied field in both temperatures (figures 6B&6D), a higher magnetization (M) value was observed for the silica-USPIO sample as compared to USPIO, suggesting that silica separating the small particles may be leading to weak ferromagnetic ordering or improving spin-ordering at the surface. Assuming

zero susceptibility of silica, the difference in saturation magnetization of the samples indicates the percent mass composition of silica, in this case, 8.4%.

To further characterize particle behavior, field cool (FC) and zero field cool (ZFC) analyses were used to determine the blocking temperature (T_B), the temperature at which material begins to demonstrate superparamagnetic behavior. For a single-domain particle in the absence of an external magnetic field, the effective magnetic anisotropy energy E_α serves as an energy barrier for blocking the flips of magnetic moments and can be approximated by:

$$E_\alpha = K_{eff} V \tag{6}$$

where K_{eff} is the effective magnetic anisotropy energy constant per unit volume, and V is the volume of magnetic nanocrystal. Thermal activation can overcome the anisotropy energy barrier when E_α becomes comparable with the thermal activation energy [22,23]:

$$K_{eff} V = \beta k_B T_B \tag{7}$$

where k_B is the Boltzmann constant, T_B is the critical blocking temperature, and the constant β, which typically varies between 25 and 34[23], represents the ratio between anisotropy and thermal energy when the relaxation time of a given particle is similar to the characteristic measuring time of the experiment. At this point, the magnetization direction flips randomly and the material becomes superparamagnetic. Relaxation, τ, is defined as

$$\tau = \tau_0 \exp(K_{eff} V / k_B T) \tag{8}$$

where τ_0 is a characteristic time related to the natural frequency of the gyromagnetic precession.

For ZFC, the sample was cooled down to 2K before applying a 0.01T field and measuring magnetization (M). The field remained constant as the temperature was increased to 370K. For FC, the temperature was first brought to 370K. The 0.01T field was then applied and held constant as susceptibility was recorded as a function of decreasing temperature (figure 7). The maximum of the ZFC graphs, typically where FC and ZFC separate, marked the blocking temperature at 162.4K for USPIO and 82.2K for silica-USPIO. This indicates silica layer deposition around individual USPIOs, which is consistent with TEM results. Interparticle separation increases in silica-coated USPIOs, thus reducing magnetic dipole–dipole interaction and decreasing the T_B. This result is typical for coated nanoparticles where the coating reduces the magnetic interaction. Kim et al [24] show similar effects for iron oxide particles covered with an oleate layer and Tartaj et al [25] show similar effects for γ-Fe_2O_3 particles dispersed in silica.

Furthermore, the USPIO ZFC curve shows a very broad maximum around 162.4K. This may indicate that the agglomeration is inhomogeneous and the different aggregates are becoming blocked at varied temperatures, creating the distribution of blocking temperatures. The silica-coated sample shows a clear peak and steeper curve indicating reduced aggregation. Also significant to note is the difference in magnitudes for the two samples. The silica-coated particles have greater magnetization which might be explained by the silica shell improving spin-ordering at the surface. That is, uncoated particles have a high degree of spin-disorder and this is reduced by having the silica coating [26,27].

4. Discussion

We have reported a rapid and economical method of synthesizing USPIOs with controlled thin coatings of silica. Industrial applications include use in power transformers, magnetic recording heads, and microwave applications. However, we have focused on optimizing the particles for medical applications. USPIOs have been widely reported as strong MRI contrast agents with high T2 relaxivity, however they need a stabilizing outer functionality. Silica improves biocompatibility and also provides a negative surface charge in physiological pH, imitating most biological species. These particles have a diameter of 20nm, making them small enough to circulate without being rapidly removed by the body [4]. Along with the advantage of small size, nanostructures derived from these silica coated USPIOs could further be directed to a specific target via the antibody-antigen recognition by conjugation of antibodies or their fragments to the outer silica surface. The particles have large surface area and can be functionalized with biomolecules (enzymes, antibodies, DNA, etc.) [28–31] and sugars (dextrans, starch, albumin, poly(ethylene glycol)) [32–34] for a variety of uses.

Furthermore, silica inhibits self-aggregation of USPIOs that could lead to ferromagnetic behavior and conserves the superparamagnetic properties of the iron oxide cores. Placing superparamagnetic iron oxide in AC magnetic fields randomly flips the magnetization direction between parallel and antiparallel orientations, a property that can be manipulated for thermotherapy in the case of drug delivery or cancer treatment. In past studies, magnetite cationic liposomal nanoparticles [35–37] and dextran-coated magnetite [38] have been shown to effectively increase the temperature of tumor cells for hyperthermia treatment for cell irradiation. Silica-coated USPIOs would also be effective in such local thermotherapy scenarios. Other medical applications of these particles include biosensors, DNA capturing, bioseparation and enzyme immobilization.

Acknowledgments

This research was supported in part by the Intramural Research Program of the NIH, National Cancer Institute, Center for Cancer Research and the British Marshall Commission.

References

1. Gupta AK, Gupta M. Biomaterials 2005;26:3995–4021. [PubMed: 15626447]
2. Shinkai M. J Bioscience Bioengineering 2002;94:606–613.
3. Wang YX, Hussain SM, Krestin GP. European Radiology 2001;11:2319–2331. [PubMed: 11702180]
4. LaConte L, Nitin N, Bao G. Materials Today 2005;8:32–38.
5. Ulman A. Chem Rev 1996;96:1533–1554. [PubMed: 11848802]
6. Mulvaney P, Liz-Marzan LM, Giersig M, Ung T. J Mater Chem 2000;10:1259–1270.
7. Liu DM, Chen IW. Acta Materialia 1999;47:4535–4544.
8. Kim DK, Mikhaylova M, Wang FH, Kehr J, Bjelke B, Zhang Y, Tsakalakos T, Muhammed M. Chemistry of Materials 2003;15:4343–4351.
9. Shen T, Weissleder R, Papisov M, Bogdanov A Jr, Brady TJ. Magnetic Resonance in Medicine 1993;29:599–604. [PubMed: 8505895]
10. Pileni MP. Nature Materials 2003;2:145–150.
11. Seip CT, O'Connor CJ. Nanostructured Materials 1999;12:183–186.
12. LaMer V, Dinegar R. Journal of American Chemical Society 1950;72:4847–4854.
13. Jolivet JP, Tronc E. Journal of Colloid and Interface Science 1988;125:688–701.
14. Bee A, Massart R, Neveu S. Journal of Magnetism and Magnetic Materials 1995;149:6–9.
15. Zhang M, Cushing BL, O'Connor CJ. Nanotechnology 2008;19:1–5. [PubMed: 19436766]
16. Homola AM, Lorenz MR, Mastrangelo CJ, Tilburg TL. IEE Trans Magn 1986;MAG-22:716.

17. Woo K, Hong J, Ahn JP. Journal of Magnetism and Magnetic Materials 2005;293:177–181.
18. Stober W, Fink A. Journal of Colloid and Interface Science 1968;26:62–69.
19. Bardosova M, Tredgold RH. Journal of Materials Chemistry 2002;12:2835–2842.
20. O'Grady K, Bradbury A. J Magn Magn Mater 1983;39:91.
21. Vroman L. Science 1974;184:585–586. [PubMed: 4821961]
22. Kumar D, Narayan J, Kvit AV, Sharma AK, Sankar J. Journal of Magnetism and Magnetic Materials 2001;232:161–167.
23. Martinez B, Roig A, Obradors X, Molins E, Rouanet A, Monty C. Journal of Applied Physics 1996;79:2580–2586.
24. Kim DK, Zhang Y, Voit W, Rao KV, Muhammed M. Journal of Magnetism and Magnetic Materials 2001;225:30–36.
25. Tartaj S, Gonzalez-Carreno T, Serna CJ. J Phys Chem B 2003;107:20–24.
26. Millan A, Urtizberea A, Silvab NJO, Palacioa F, S Amaralb V, Snoeckc E, Serinc V. Journal of Magnetism and Magnetic Materials 2007;312:L5–L9.
27. Shendruk TN, Desautels RD, Southern BW, Lierop Jv. Nanotechnology 2007;18:455704.
28. Luckarift HR, Spain JC, Naik RR, Stone MO. Nature Biotechnology 2004;22:211–3.
29. Qhobosheane M, Santra S, Zhang P, Tan W. Anaylst 2001;126:1274–1278.
30. Santra S, Zhang P, Wang KM, Tapec R, Tan WH. Analytical Chemistry 2001;73:4988–4993. [PubMed: 11681477]
31. Kneuer C, Sameti M, Haltner EG, Schiestel T, Schirra H, Schmidt H, Lehr C-M. International Journal of Pharmaceutics 2000;196:257–261. [PubMed: 10699731]
32. Santarelli A, Muller D, Jozefonvicz J. J Chromatogr 1988;443:55–62. [PubMed: 2459150]
33. Kim J, Somorjai GA. J Am Chem Soc 2003;125:3150–3158. [PubMed: 12617683]
34. Lesot P, Chapuis S, Bayle J, Rault J, Lafontaine E, Campero A, Judeinstein P. J Mater Chem 1998;8:147–151.
35. Schneider S, Rusconi S. Biotechniques 1996;21:876–880. [PubMed: 8922629]
36. Yanase M, Shinkai M, Honda H, Wakabayashi T, Yoshida J, Kobayashi T. Jpn J Cancer Res 1997;88:630–632. [PubMed: 9310134]
37. Yanase M, Shinkai M, Honda H, Wakabayashi T, Yoshida J, Kobayashi T. Jpn J Cancer Res 1998;89:463–469. [PubMed: 9617354]
38. Chan DCF, Kirpotin DB, Bunn PA. J Magn Magn Mater 1993;122:374–378.

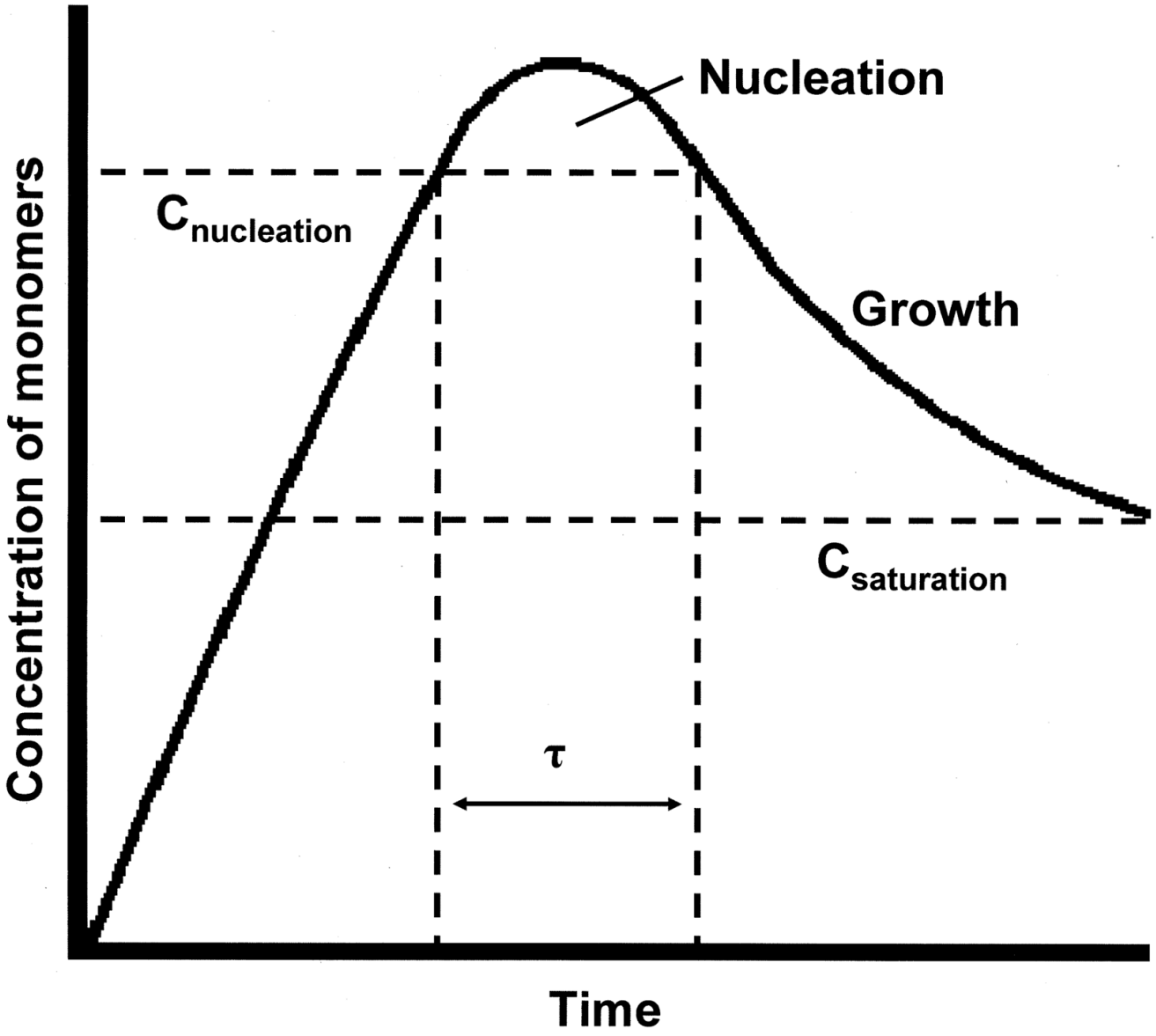

Figure 1.
LaMer Diagram illustrating the time dependence of monomers to form monodisperse colloids.

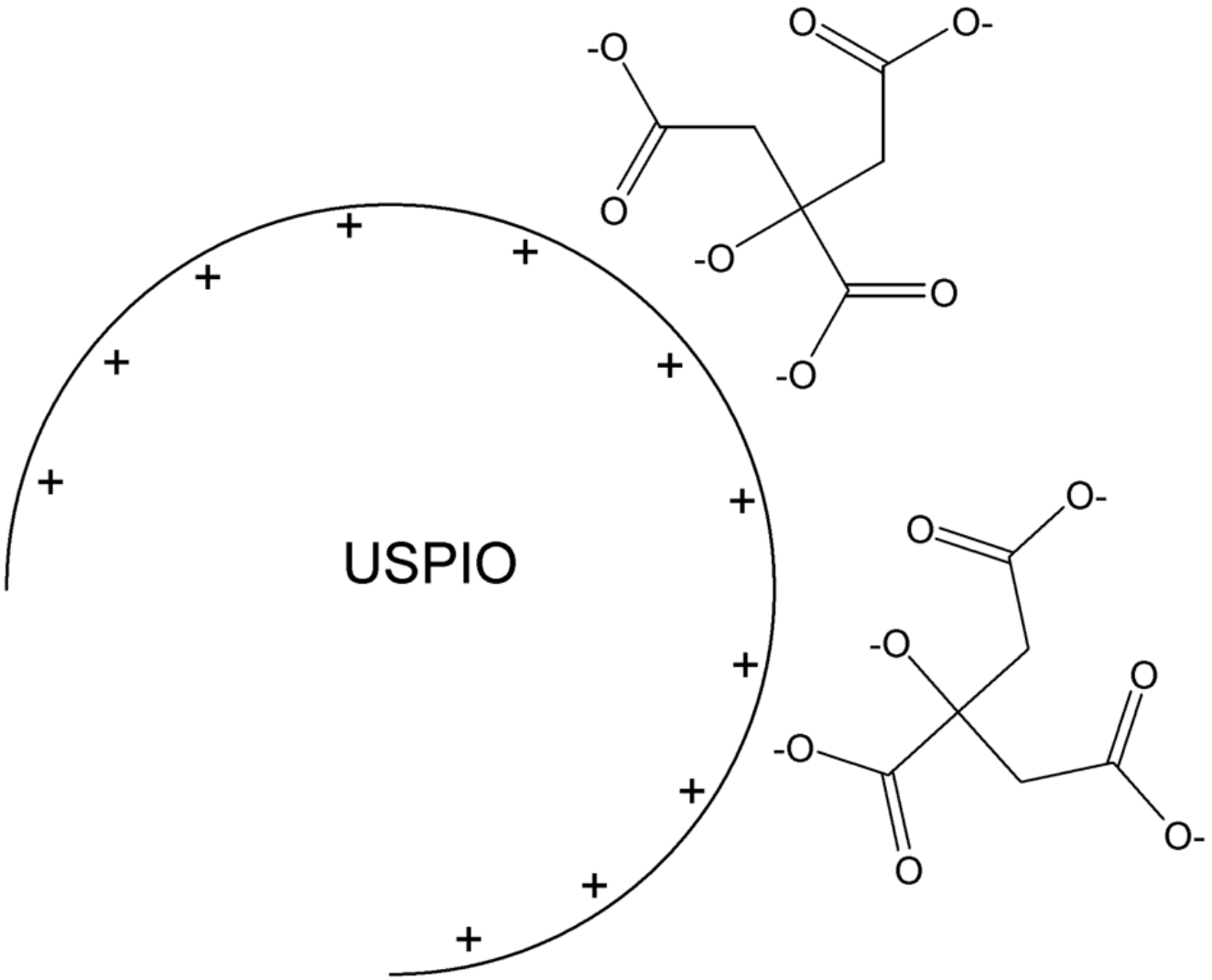

Figure 2.
Citrate-complexed USPIO.

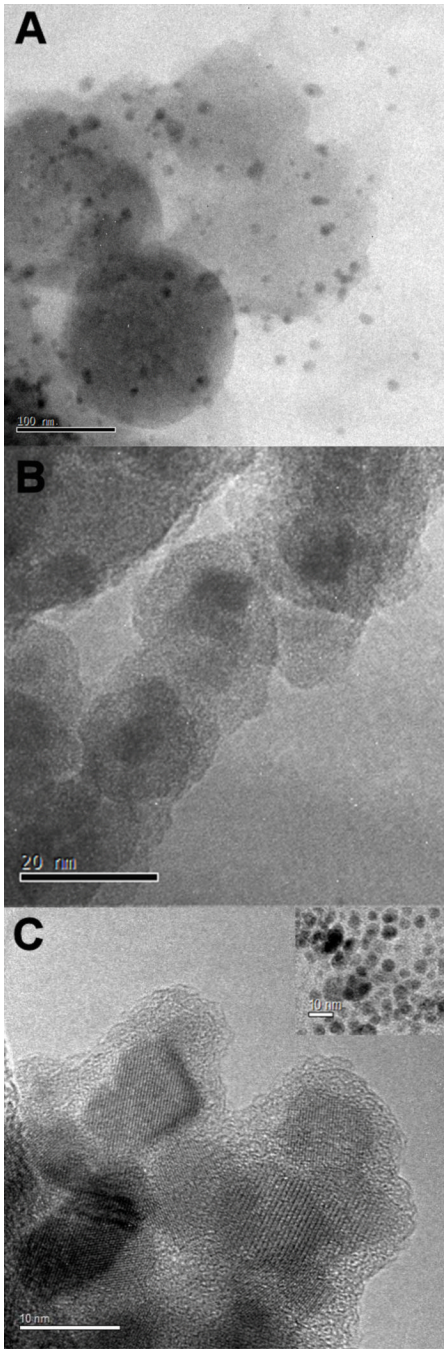

Figure 3.
TEM using a JEOL 4000EX of synthesized (A) ~175nm silica beads embedded with USPIOs, (B) USPIOs coated with ~10nm-thick shells of silica, and (C) USPIOs coated with ~2.5nm-thick shells of silica.

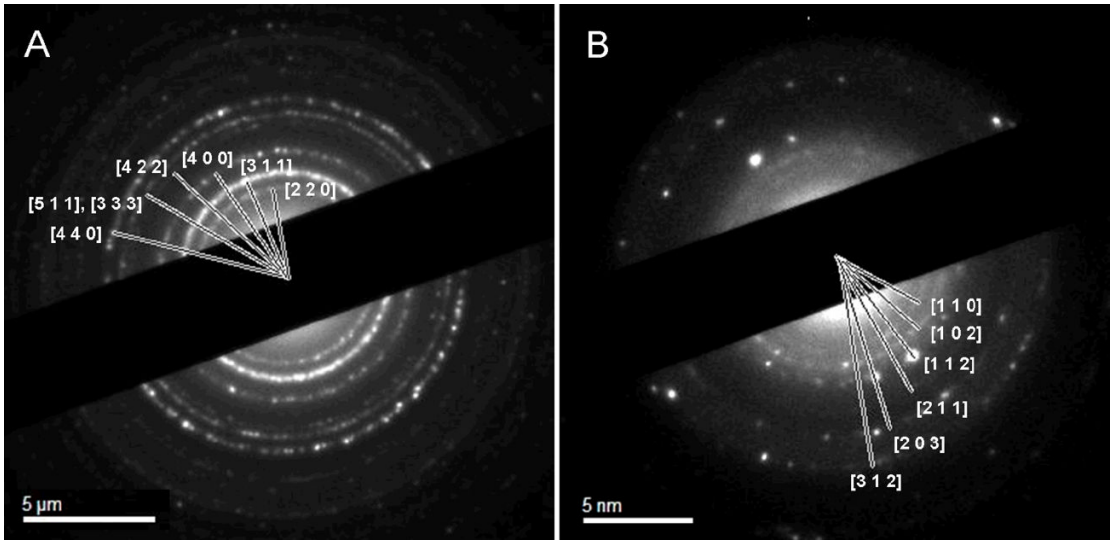

Figure 4.
Diffraction patterns using JEOL 4000EX of silica-coated USPIOs: (A) magnetite/maghemite core, and (B) silicon(IV) oxide outer shell.

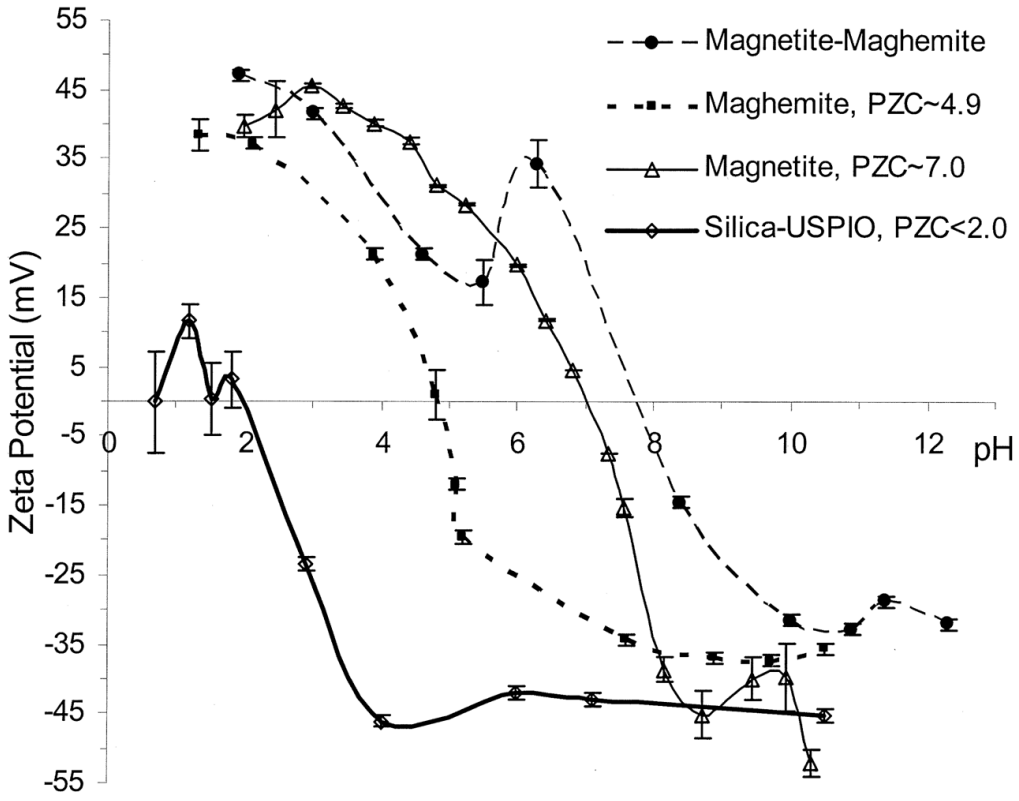

Figure 5.
Surface charge characterization of particles in water.

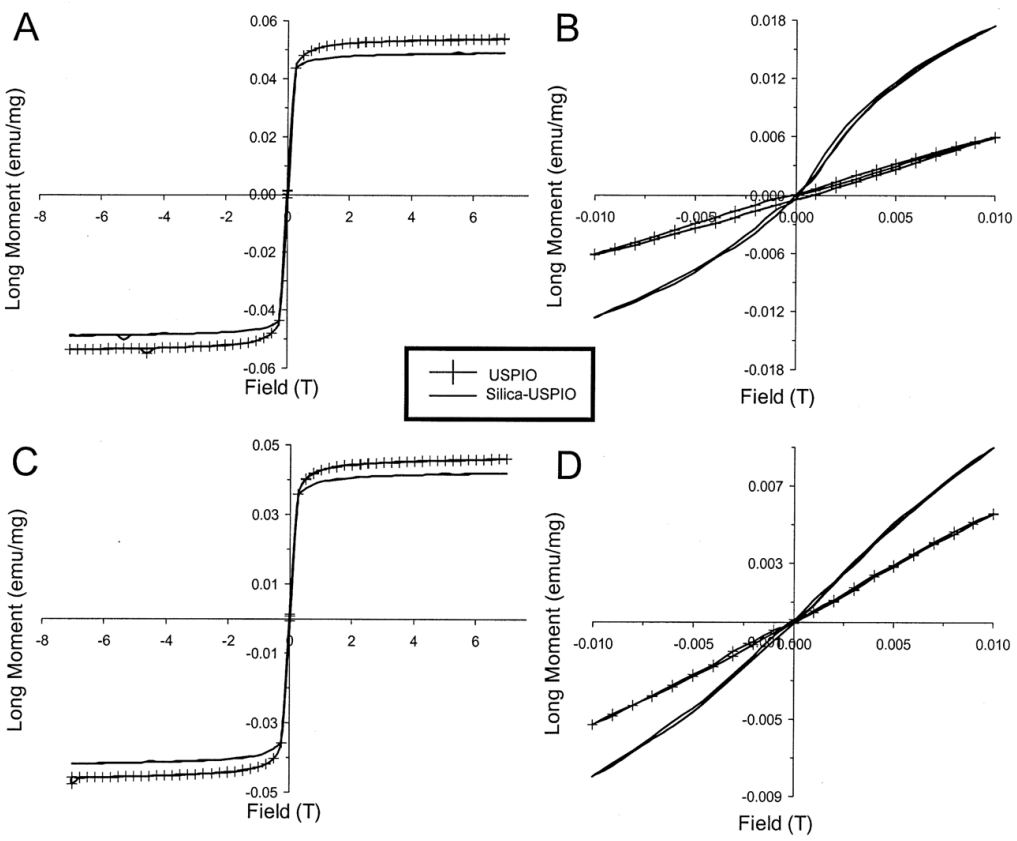

Figure 6.
Magnetization versus applied field of USPIO and silica-coated USPIOs measured at (A) T=100K (±7 T), (B) T=100K (±0.1 T), (C) T=310.15K (±7 T), and (D) T=310.15K (±0.1 T).

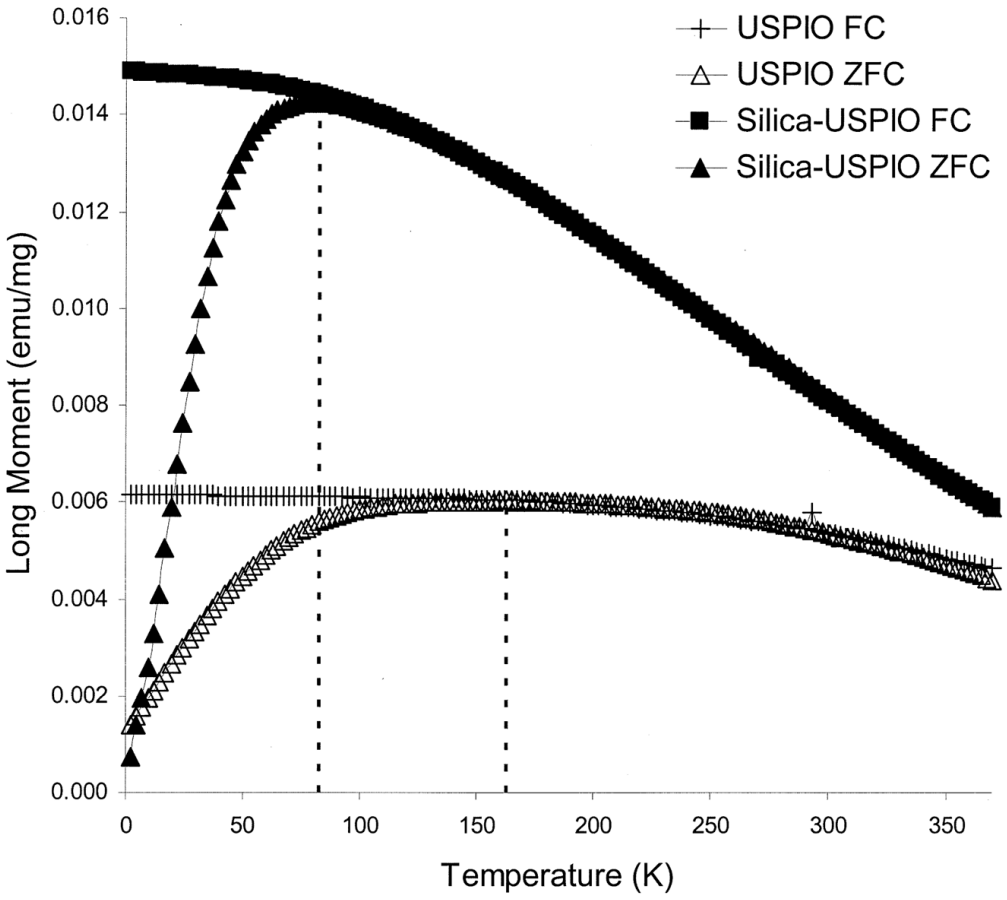

Figure 7.
Temperature dependence of the magnetization (ZFC & FC) of USPIO and Silica-USPIO at H=0.01T.